LOW-x QCD AT THE LHC WITH THE ALICE DETECTOR*

Magdalena Malek

for the ALICE Collaboration

Institut de Physique Nucléaire d'Orsay (IPNO)
CNRS UMR8608–IN2P3, Université Paris Sud-XI, Paris, France
Magdalena.Malek@cern.ch

(Received October 30, 2009)

We give a brief review of the physics of gluon saturation and non-linear QCD evolution at small value of the Bjorken-x variable. We discuss the ALICE capability for low-x studies at the LHC. In particular, we concentrate on the heavy quark production in the CGC framework and its observation with the ALICE Muon Spectrometer.

PACS numbers: 25.75.–q, 14.65.Fy, 14.65.Dw

1. Heavy quark production cross-section

The heavy quark production cross-section in H_1–H_2 collisions can be illustrated by the formula:

$$\sigma^{H_1,H_2} = \sum_{i,j} \int dx_1 dx_2 f_i(x_1)^{H_1} f_j(x_2)^{H_2} \sigma_{ij}(x_1, x_2, s)\,, \tag{1}$$

where $\sigma_{ij}(x_1, x_2, s)$ is the perturbative partonic cross-section for two hard-scattering to produce a pair of heavy quarks which depends in particular on the available energy. This parton level cross-section is calculable as a power series in the strong coupling $\alpha_{\rm s}$ which depends on the renormalisation scale. The nucleon Parton Distribution Functions (PDF) $f_{i/j}(x_1/x_2)^{H_1/H_2}$ gives the probability to find the parton i/j in a nucleon of type H_1/H_2 as a function of fraction x_1/x_2 of the nucleon's momentum carried by the parton. The PDFs are non-perturbative objects and thus cannot be calculated from first

* Presented at the International Meeting "Excited QCD", Zakopane, Poland, February 8–14, 2009.

principles. They are extracted from the structure functions of the nucleon in deep inelastic scattering (DIS) experiments. The comprehension of PDFs is mandatory to make any predictions about the heavy flavor production.

2. Parton structure and evolution equations

2.1. Parton distribution in linear regime

The DGLAP (Dokshitzer–Gribov–Lipatov–Altarelli–Parisi) [1] evolution equation applicable in the Bjorken limit ($Q^2 \to \infty$ and fixed x) takes into account the Q^2 dependence of the PDFs. It allows a resummation of leading powers of $[\alpha_{\rm s} \ln(Q^2)]^n$ generated by a parton cascade in a region of the phase space where the transverse momenta of gluons is strongly ordered: $Q^2 \gg k^2_{n{\rm t}} \gg k^2_{(n-1){\rm t}} \gg \ldots \gg k^2_{1{\rm t}}$. In this approach the transverse momenta of the initial partons are neglected.

At high energy (or decreasing x), the probability of gluon emission increases as $\alpha_{\rm s} \ln(1/x)$. In this regime, the transverse momenta of the partons are of the same order of magnitude than the longitudinal ones and thus have to be taken into account in the reaction dynamics description. When the gluon density $\mathcal{N}$ is not too high, the modification of the gluon distribution with increasing energy can be described by the BFKL (Balitsky–Fadin–Kuraev–Lipatov) evolution equation [2]. This equation can be used in the Regge limit ($s \to \infty$ and fixed Q^2) of QCD. The PDFs are described in terms of $k_{\rm t}$-unintegrated PDFs $\phi(x, k_{\rm t})$ related to the usual gluon distribution $xg(x, Q^2)$ by $xg(x, Q^2) \sim \int_0^{Q^2} d^2 k_{\rm t} \phi(x, k_{\rm t})$. This is essentially a linear equation and its solution at asymptotically large energies shows an exponential growth of the number of gluons. This unlimited growth of the gluon density leads ultimately to a violation of the unitarity bound for the cross-section. The BFKL equation must be modified so as not to violate the unitarity.

2.2. Non-linear evolution and parton saturation

At some small enough value of x, the gluon density is so large that the non-linear gluon recombination becomes important. The gluon density per unit area of the nucleus with atomic number A is $\rho_A \sim xg_A(x, Q^2)/A^{2/3}$ and the gluon recombination cross-section is $\sigma_{gg \to g} \sim \alpha_{\rm s}/Q^2$. The border line between the linear and non-linear regimes is given by the saturation scale $Q_{\rm s}$ satisfying $\rho_A \sigma_{gg \to\, g} = 1$. The gluon recombination becomes important when $\rho_A \sigma_{gg \to\, g} > 1$ thus $Q^2 \leq Q^2_{\rm s}$ with $Q^2_{\rm s} \sim \alpha_{\rm s} x g_A(x, Q^2_{\rm s})/A^{2/3}$. Partons with $Q^2 > Q^2_{\rm s}$ are not affected by saturation, evolution goes towards the dilute system, and can be described by DGLAP or BFKL equations. On the other hand, partons with $Q^2 < Q^2_{\rm s}$ are in the saturation regime and

their evolution is described by the non-linear JIMWLK (Jalilian Marian–Iancu–McLerran–Weigert–Leonidov–Kovner) equation [3]. This equation can be schematized by:

$$\frac{\partial \mathcal{N}(k_{\mathrm{t}}, y)}{\partial y} \simeq c_1 \mathcal{N}(k_{\mathrm{t}}, y) - \alpha_{\mathrm{s}} c_2 \mathcal{N}^2(k_{\mathrm{t}}, y)\,, \tag{2}$$

with rapidity $y \equiv \log(1/x)$ and constant parameters $c_{1,2}$ of the order of one. One remarks that the gluon recombination (or quadratic term) becomes important when $\mathcal{N}$ reaches $1/\alpha_{\mathrm{s}}$. The gluon production stops growing, this is the so-called gluon saturation. The saturation phenomena can be described by an effective theory: the Color Glass Condensate (CGC). The CGC is a new form of nuclear matter which controls hadronic interactions at asymptotically large energies. The origin of the name is the following. First of all, the CGC is made of small-x gluons which carry the *color* charge. Next, these small-x gluons are created by partons with larger x which act as a frozen color sources, *glass*, for the emission of small-x gluons. Lastly, *condensate* because the soft degrees of freedom are as densely packed as they can.

3. Low-x QCD studies at the LHC with the ALICE

The LHC (Large Hadron Collider) at CERN will provide, at nominal operating conditions, p+p, p+Pb and Pb+Pb collisions at $\sqrt{s_{NN}} = 14$, 8.8 and 5.5 TeV, respectively, with luminosities $\mathcal{L} \sim 10^{34}$, 10^{29} and $5 \times 10^{26}\,\mathrm{cm}^{-2}\mathrm{s}^{-1}$. These conditions allow to access unprecedentedly low values of the Bjorken-x variable. The copious production of heavy quarks (charm and beauty) can be used as a probe of low-x QCD phenomena. At LHC energies heavy quarks are mainly produced through gluon–gluon fusion processes thus their production cross-sections are significantly affected by parton dynamics in the small-x regime.

ALICE (A Large Ion Collider Experiment) [4] is the experiment dedicated to study the properties of matter created in Pb+Pb collisions at the LHC. The detector contains a wide array of sub-detectors for measuring

TABLE I

Bjorken-x values for charm and beauty production at central rapidity and $p_{\mathrm{t}} = 0$ at SPS, RHIC and LHC energies. Table extracted from [4].

Machine	SPS	RHIC	LHC	LHC
System	Pb+Pb	Au+Au	Pb+Pb	$p+p$
Energy (GeV)	17	200	5500	14000
$c\bar{c}$	$x \simeq 10^{-1}$	$x \simeq 10^{-2}$	$x \simeq 4 \times 10^{-4}$	$x \simeq 2 \times 10^{-4}$
$b\bar{b}$	—	—	$x \simeq 2 \times 10^{-3}$	$x \simeq 6 \times 10^{-4}$

hadrons, leptons and photons. Table I shows the x regimes for the production of $c\bar{c}$ and $b\bar{b}$ pairs at SPS, RHIC and LHC (for ALICE) energies. As we can see in Table I the increase of the collision energy involves the decrease of the value of the Bjorken-x.

3.1. Simulations: setup

The simulation of the heavy quark production within the CGC framework are performed with the AliRoot [5] simulation code. The theoretical ingredients (PDF and partonic cross-section) of Eq. (1) for each approach are discussed in next sections. The results are compared to the reference simulations for the ALICE experiment (PYTHIA) that are based on the Mangano–Nason–Ridolfi (MNR) calculation [6]. The comparison between $p + p$ and Pb+p collisions allows to draw preliminary conclusions about the CGC observation with the ALICE muon spectrometer [7] covering the forward pseudo-rapidity region $(-4 \leq \eta \leq -2,5)$.

Collinear factorization: PYTHIA tuned to MNR

- $p+p$ collisions are simulated with PYTHIA tuned to reproduce heavy quark production cross-section obtained with MNR calculation. The CTEQ [8] parametrization of the proton PDF is used.

- Pb+p collisions are simulated from $p+p$ ones using Glauber geometric model allowing to calculate the number of binary collisions. Shadowing effects in the gluon distribution are added by hand, by using a nuclear modification factor. This factor, not well known at LHC energies, can be calculated using different parametrization methods. In this study we used the EKS98 parametrization [9]. Within this model, the transverse momentum k_{t} of partons is given by means of a Gaussian distribution with a zero mean value and a width ($\sigma = \mid k_{\mathrm{t}} \mid$) that depends on the considered flavor and the colliding system. For $p + p$ and Pb+p collisions, this parameter is respectively fixed to 1 and 1.16 GeV/c for charm, and 1 and 1.6 GeV/c for beauty.

CGC approach

In this approach the proton PDF is given by the non-saturated CTEQ parametrization. The lead structure is described by the PDF taking into account the saturation effects. More precisely, it contains the multiple scattering corrections in the partonic cross-section and the non-linear terms of the JIMWLK equation. The initial condition for the JIMWLK equation is calculated for $x = 10^{-2}$ using the McLerran–Venugoplan model [10].

3.2. Results on heavy quarks level

We calculate the charm and beauty production cross-section and their ratios for both approaches. The ratio $R_{\mathrm{Pb}p} = (dN_{\mathrm{Pb}p}/dydp_{\mathrm{t}})/(N_{\mathrm{coll}}dN_{pp}/dydp_{\mathrm{t}})$ defines the nuclear modification factor that can be calculated from experimental data. The results are given in Table II. One remarks that the values of shadowing factors for beauty are very close in both models. For charm, these factors are very different. It shows that the gluon recombination effects are more important in the CGC approach that in the MNR one. In fact, the $c\bar{c}$ pairs are produced, on average, by fusion of gluons at smaller x than the ones producing the $b\bar{b}$ pairs ($x = (M_{Q\overline{Q}})/(\sqrt{s_{NN}})\exp(\pm y_{Q\overline{Q}})$). Since small-$x$ gluons are more sensitive to recombination effects, this are more visible in the charm case.

Table II gives also the cross-section ratios for beauty over charm production. One sees that the MNR approach always predicts a ratio smaller than 5%, whereas the CGC approach gives a ratio larger than 10%.

TABLE II

Production ratios of charm and beauty in Pb+p collisions at $\sqrt{s_{NN}} = 8.8$ TeV normalized to the number of binary collisions N_{coll} and cross-section ratios between beauty and charm for rapidity $y < 0$ in MNR and CGC approaches.

Approach	$dN^{c\bar{c}}_{\mathrm{Pb}p}/dN^{c\bar{c}}_{pp}$	$dN^{b\bar{b}}_{\mathrm{Pb}p}/dN^{b\bar{b}}_{pp}$	$dN^{b\bar{b}}_{pp}/dN^{c\bar{c}}_{pp}$	$dN^{b\bar{b}}_{\mathrm{Pb}p}/dN^{c\bar{c}}_{\mathrm{Pb}p}$
MNR with EKS98	0.77	0.85	0.03	0.04
CGC	0.60	0.80	0.10	0.14

The evolution of the nuclear modification factor $R_{\mathrm{Pb}p}$ as a function of transverse momentum and rapidity is presented in Fig. 1. One remarks that below ~ 4 GeV/c, in the CGC approach, the depletion for charm is much more important than for beauty. It can be understood by recombination

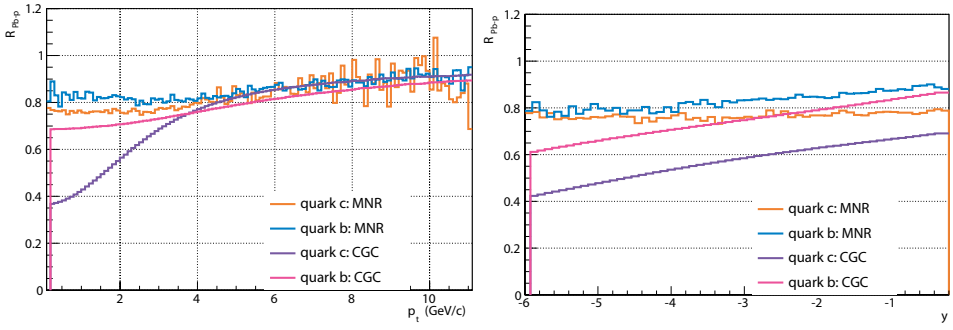

Fig. 1. $R_{\mathrm{Pb}p}$ ratios as a function of p_{t} (left part) and rapidity (right part).

and multiple scattering of small-x gluons which are responsible for charm production. This effect is less pronounced in the MNR + EKS98 approach. Shadowing effects are also visible from the rapidity dependence of $R_{\mathrm{Pb}p}$. Both approaches show the decrease of this ratio at high rapidities but it is clearly more noticeable, for both flavors, in the CGC approach.

3.3. Results on hadron and muon level

Next, the quark fragmentation into heavy hadrons was performed. The decay of produced hadrons through their semi-muonic channel was applied. Finally, the transport of produced muons through the muon spectrometer was completed [11]. It is important to highlight that a full AliRoot simulation was used to transport particles and to reconstruct their tracks; thus a realistic signal generation from the full detector response and a complete clustering and tracking procedure were applied.

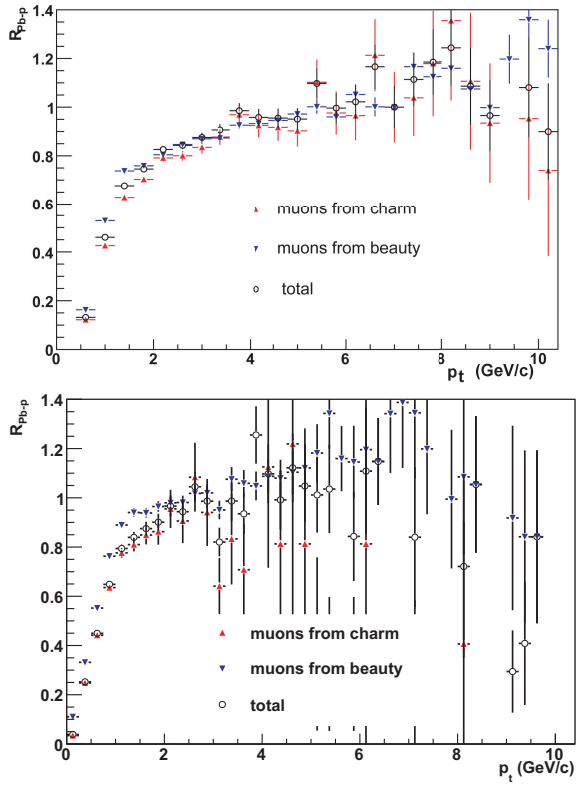

Fig. 2. $R_{\mathrm{Pb}p}$ ratio for muons from charm and beauty reconstructed in the ALICE muon spectrometer. The top (bottom) plot corresponds to the results obtained with the CGC (MNR) model.

Reconstructed single muon spectra are studied in this part. The shift of the center of mass frame with respect to the laboratory one, by $\delta y = 0.47$ for Pb $+p$ collisions, is taken into account. This kinematical shift constrains the rapidity window where the $R_{\mathrm{Pb}p}$ can be measured; the ratio will correspond to muons with $y \in [-2.97, -4]$ for $p + p$ collisions and muons with $y \in [-2.5, -3.53]$ for Pb$+p$ collisions.

The ratio $R_{\mathrm{Pb}p}$, presented in Fig. 2 as a function of p_{t} for muons from charm and beauty exhibits a similar behavior for both flavours in the two models. The observation of the saturation effects via the $R_{\mathrm{Pb}p}$ ratio will be difficult at low p_{t} ($p_{\mathrm{t}} < 2\,\mathrm{GeV}/c$) in the ALICE muon spectrometer due to the different experimental cuts.

4. Conclusions

The main purpose of this work was to investigate the predictions of the CGC approach in the case of the charm and beauty production rates for ALICE experiment. The results were compared to the reference simulations of ALICE which are based on the MNR calculation. It was observed that the heavy quark production is affected by the small-x effects in the low p_{t} region. It was shown that the shadowing effects are much more significant in the case of the CGC approach. It was also seen that the Cronin effect is very important in the CGC framework, especially for the charm which is more affected because of its smaller mass.

The muon level results were obtained from realistic simulations containing the muon spectrometer response function. Finally, we conclude that to observe experimentally the small-x effects with the muon spectrometer of the ALICE detector a very challenging analysis has to be done.

REFERENCES

[1] V.N. Gribov, L.N. Lipatov, *Sov. J. Nucl. Phys.* **15**, 438 (1972); G. Altarelli, G. Parisi, *Nucl. Phys.* **B126**, 298 (1977); Yu.L. Dokshitzer, *Sov. Phys. JETP* **46**, 641 (1977).

[2] L.N. Lipatov, *Sov. J. Nucl. Phys.* **23**, 338 (1976); E.A. Kuraev, L.N. Lipatov, V.S. Fadin, *Zh. Eksp. Teor. Fiz.* **72**, 3 (1977) (*Sov. Phys. JETP* **45**, 199 (1977)); Ya.Ya. Balitsky L.N. Lipatov, *Sov. J. Nucl. Phys.* **28**, 822 (1978).

[3] E. Iancu, R. Venugopalan, `hep-ph/0303204`.

[4] [ALICE Collaboration], *J. Phys. G* **32**, 1295 (2006).

[5] `http://aliceinfo.cern.ch/Offline/AliRoot/Manual.html`

[6] M.L. Mangano, P. Nason, G. Ridol, *Nucl. Phys.* **B373**, 295 (1992).

[7] [ALICE Collaboration], *JINST* **3**, S08002 (2008); [ALICE Collaboration], CERN/LHCC **99**, (1999); [ALICE Collaboration], CERN/LHCC **2000-046**, (2000).

[8] J. Pumplin, A. Belyaev, J. Huston, D. Stump, W.K. Tung, *J. High Energy Phys.* **0602**, 032 (2006).

[9] K.J. Eskola, V.J. Kolhinen, C.A. Salgado, *Nucl. Phys.* **A661**, 645 (1999).

[10] L.D. McLerran, R. Venugopalan, *Phys. Rev.* **D49**, 2233 (1994).

[11] L. Aphecetche *et al.,* ALICE-Note to be published.